OBSERVED AND SIMULATED GROUND MOTIONS IN THE GUBBIO BASIN, CENTRAL ITALY DURING THE M_W5.7 1984 EARTHQUAKE

Abraham Jetson Ronald
ROSE School, IUSS-Pavia, Italy

Chiara Smerzini
Department of Structural Engineering, Politecnico di Milano, Italy

SUMMARY:
The main aim of this work is to illustrate the main results obtained through 3D numerical simulations of long period earthquake ground motion within the Gubbio plain, a closed-shape alluvial basin located in the Central Italy, during the M_w 5.7 Gubbio earthquake on 29th April 1984. The numerical model, discretized by means of spectral elements, was designed to propagate up to frequencies of about 2 Hz, including a realistic description of the Gubbio plain and of the seismogenic source as well. The simulated waveforms were found to be in reasonable agreement with strong motion recordings. Results of numerical simulations inside the alluvial basin were analyzed to shed light on complex phenomena of seismic wave propagation related to basin-edge induced surface wave propagation and on their possible dependence on source parameters.

Keywords: numerical simulation, complex site effects, surface waves

1. INTRODUCTION

Intramountain alluvial basins are a typical surface expression of extensional tectonic activity in some of the Italian regions with greater seismic hazard, in particular in the Central and Southern Apennines. Features common to these basins are the closed and often elongated shape in the direction of the mountain chain, the relatively small spatial extent (few tens of km) and the presence of active fault systems bordering the basins, capable of producing earthquakes up to magnitude about 7.

It is widely recognized that earthquake ground motion within complex geological structures, such as sedimentary basins or alluvial fans (Koketsu and Miyake, 2008) and in the near-source region (Archuleta and Hartzell, 1981; Bray and Rodriguez-Marek, 2004; Somerville et al, 1997) displays peculiar features in terms of amplitude, duration and frequency content. In such conditions, standard methods for earthquake ground motion prediction, based on the assumptions of vertical plane wave propagation in horizontally layered media, are generally inadequate, since they cannot reproduce complex phenomena of seismic wave propagation associated, on one side, with source kinematics and rupture directivity and, on the other side, with the complex morphology of the basin, such as resonance phenomena and basin-edge induced surface waves.

The Gubbio plain, located in the Umbria-Marche Appenines (Central Italy), is a 22 km long basin, aligned along the NW-SE direction, with a maximum width of approximately 5 km near the town of Gubbio and a maximum thickness of about 600 m (Fig. 1.1). We refer the reader to Bindi et al. (2009) for a careful review of the in-situ geophysical investigations performed in recent years for the seismic characterization of the Gubbio basin.

The Gubbio area is characterized by relatively moderate seismicity, mainly related to the Umbria fault system. The strongest instrumental earthquake in the Gubbio area occurred on April 29th 1984 with moment magnitude M_W = 5.7. The basin is bordered to the east for its entire length by the Gubbio Fault, part of the Umbria-Marche fault system, which is recognized as an active fault (Pucci et al., 2003). In the middle part of the Gubbio fault there is a bend which may act as a geometric barrier during the propagation of earthquake rupture. This is the reason why two distinct segments of the Gubbio fault, namely, Gubbio South and Gubbio North, are identified in the Database of Individual

Seismogenic Sources DISS3 (DISS Working Group, 2009), a georeferenced repository of seismogenic sources for Italy.
Instrumental and historical data suggest that the 1984 Gubbio earthquake was originated by the Southern segment of the Gubbio fault (identified as ITGG037 in the DISS3 database), hence implying that rupture propagated towards the north and the fault bend acted as a barrier to rupture propagation (Collettini et al., 2003). The unbroken northern segment remains a potential seismic source for a future M_W 6 earthquake.

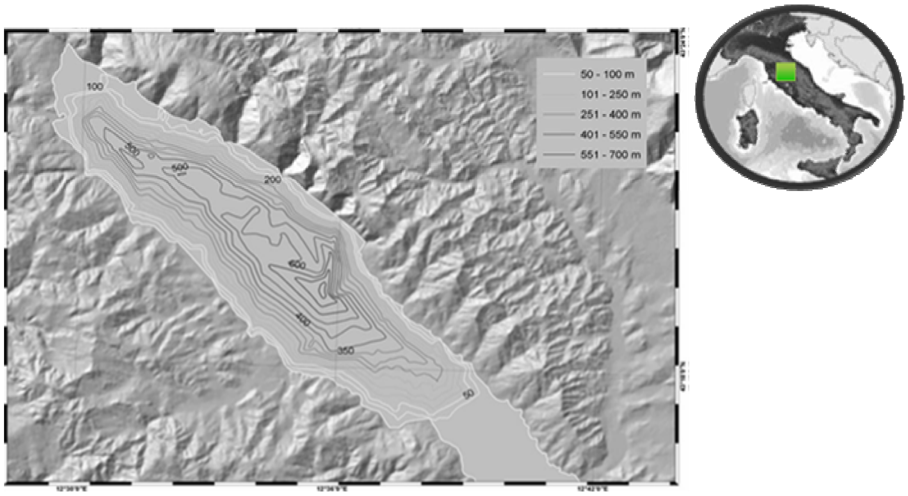

Figure 1.1. Gubbio basin (Central Italy): contour lines of the bedrock submerged topography (from Bindi et al. 2009).

2. NUMERICAL MODEL FOR THE 1984 EARTHQUAKE SCENARIOS

In this section we aim at illustrating the main features of the 3D numerical simulations carried out to simulate the M_W 5.7 1984 Gubbio earthquake scenarios. To this end the spectral element method proposed by Faccioli et al. (1997) and implemented in the computer code *GeoELSE* (*GeoELastodynamics by Spectral Elements*, http://geoelse.stru.polimi.it) has been used. GeoELSE is a numerical code for simulation of linear and non linear elastic wave propagation in heterogeneous media, based on the spectral elements (Stupazzini et al., 2009). With this code, realistic topography and complex subsurface structures have been efficiently incorporated.
A 3D hexahedral spectral element mesh was designed to propagate up to frequencies of about 2 Hz, including the following features: (a) a kinematic source model for the Gubbio South fault; (b) a 3D model of the Gubbio plain; (c) a layered deep crustal model;(d) a linear visco-elastic material behavior with a Q factor proportional to frequency.
Referring to the source model, we adopted the kinematic fault solution proposed by Ameri et al. (2010) as "best-fit" model for the 1984 earthquake magnitude (Tab. 2.1). Ameri et al. (2010) investigated through massive parametric numerical analyses the effect of variability in the kinematic definition of the source on earthquake ground motion with application to the 1984 Gubbio earthquake. In this work they found that the best fit seismic source model is given by a rupture propagating with velocity V_R = 2.65 km/s from a hypocenter located approximately at the center of the fault, leading to a bilateral propagating rupture. The adopted slip distribution model, corroborated by Ameri et al. (2010), is shown in Fig. 2.1 (right-hand side)
Three scenario events, referred to as S1, S2 and S3, were simulated by varying the hypocenter location and the rise time τ_R, namely: S1) the hypocenter is located approximately at the center of the fault and a constant value of τ_R = 1.0 s is assumed; S2) the hypocenter location is shifted to the bottom of the fault and the same rise time τ_R = 1.0 s as for S1 is assumed; S3) same hypocenter location as for S1 but τ_R = 0.8 s.
Following Smerzini et al. (2011), a simplified model of the Gubbio plain was defined, considering the

3D shape of the alluvial cover, as retrieved from the available geophysical investigations (see Fig. 1.1), and an average soil profile defined as follows:

$$V_P(z) = 1000+30\,z^{1/2}\ ;\ V_S\,(z) = 250+30z^{1/2}\ ;\ \rho = 1900 \text{ and } Q_S = 50 \qquad (2.1)$$

where V_P and V_S are the P- and S-wave velocity (in m/s), respectively, ρ is the mass density (in kg/m^3), and Q_S is the S-wave quality factor at 1 Hz. Such simplified homogenous model was adopted keeping in mind the feasibility of computational demand. Instead, a 1D velocity profile was assumed for the deep crustal structure, as listed in Tab. 2.2.
Fig. 2.1 (left-hand-side) shows the computational grid adopted for the simulation of the Gubbio earthquake scenarios. The model covers a total volume of about 78x53x10 km^3 and is discretiszed using an unstructured hexahedral mesh with characteristic element size ranging from ~ 100 m within the Gubbio basin and ~ 900 m in the bottom layers. Note that the mesh has been designed to follow the surface topography, as derived from a 250 m resolution digital elevation model (DEM). The time step for explicit second-order finite difference time integration scheme is Δt = 0.0003 s. Numerical simulations were carried out on the Lagrange cluster located at *CILEA* (http://www.cilea.it/), resulting in a total computer time of about 60 hours with 62 CPUs for a 60 s simulation.

Table 2.1. Source parameters for the 1984 Gubbio earthquake. From Ameri et al. (2010):

Hypocenter (Lat, Long)	**Length (km)**	**Width (km)**	**Min depth (km)**	**strike (°)**	**dip (°)**	**rake (°)**	**V_R (km/s)**
(43.2284 °N, 12.5559 °E)	8	6	4.3	130	20	270	2.56

Table 2.2. Layered crustal model, from top (ground surface) to bottom. Adapted from Hernandez et al. (2004) and Mirabella et al. (2004).

Layer	***H* (m)**	**V_P (m/s**	**V_S (m/s)**	**ρ (kg/m^3)**	**Q_S**
B1	1100	3500	1800	2200	80
B2	1586	4000	2200	2400	100
B3	1000	4800	2666	2600	150
B4	3000	5500	3055	2800	250
B5	3314	6300	3500	2900	300

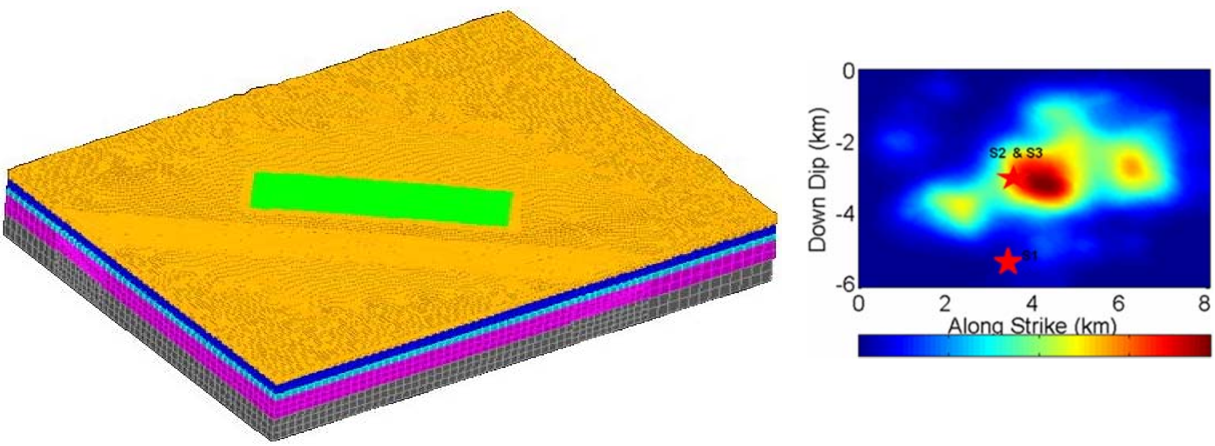

Figure 2.1. Left: 3D hexahedral spectral element mesh adopted for the simulation of the Gubbio earthquake scenarios. Right: fault slip distribution (from Ameri et al., 2010). The red star denotes the location of the hypocenter used for different scenarios.

3. COMPARISON WITH STRONG MOTION RECORDINGS

Three accelerometric stations of the Italian strong motion network, namely GBB, NCR, and UMB (see ITACA database: http://itaca.mi.ingv.it), were triggered by the 1984 Gubbio earthquake. Unfortunately none of these strong motion stations is located in the basin, but that is not a setback for the present study because the accuracy of simulated seismic surface motions in the basin has been already verified against strong motion recordings by Smerzini et al. (2011). Taking advantage of the spectral element approach, the usable frequency range of the synthetic waveforms reaches the upper limit f_{max} = 2 Hz. Nevertheless, due to the limited reliability of the analog instruments, the recordings were high-pass filtered at 0.40 Hz, so that the comparison between simulated and synthetic waveforms will be shown in the frequency range 0.40 – 2.0 Hz.

To provide a quantitative evaluation of the performances of numerical simulations with respect to several measures of ground motion shaking, ten different parameters of earthquake ground motion were used for comparison between observed and simulated waveforms, namely, peak ground acceleration (PGA), peak ground velocity (PGV), peak ground displacement (PGD), significant duration, Arias intensity, the integral of velocity squared (energy), cumulative absolute velocity, pseudo spectral acceleration (PSA), pseudo spectral velocity (PSV), spectral displacement (SD). Each parameter is compared on a scale from 0 to 10, with 10 giving perfect agreement. Scores for each parameter were estimated as proposed by Anderson (2004): a score below 4 is a poor fit, a score of 4 to 6 is a fair fit, a score of 6 to 8 is a good fit, and a score over 8 is an excellent fit. We underline that we did not use the same parameters as suggested by Anderson (2004) but we followed the same approach. The similarity of recorded and simulated waveforms at three stations, as estimated using the Anderson's criteria, is displayed in Fig. 3.1 for the three scenarios under consideration. It turns out that scenario S2 has the largest goodness-of-fit parameters for all stations. In particular, for S2, referring to the GBB station, almost all ground motion parameters except duration are in satisfactory agreement with the observations, and, interestingly, for all three stations, the spectral response parameters have good scores.

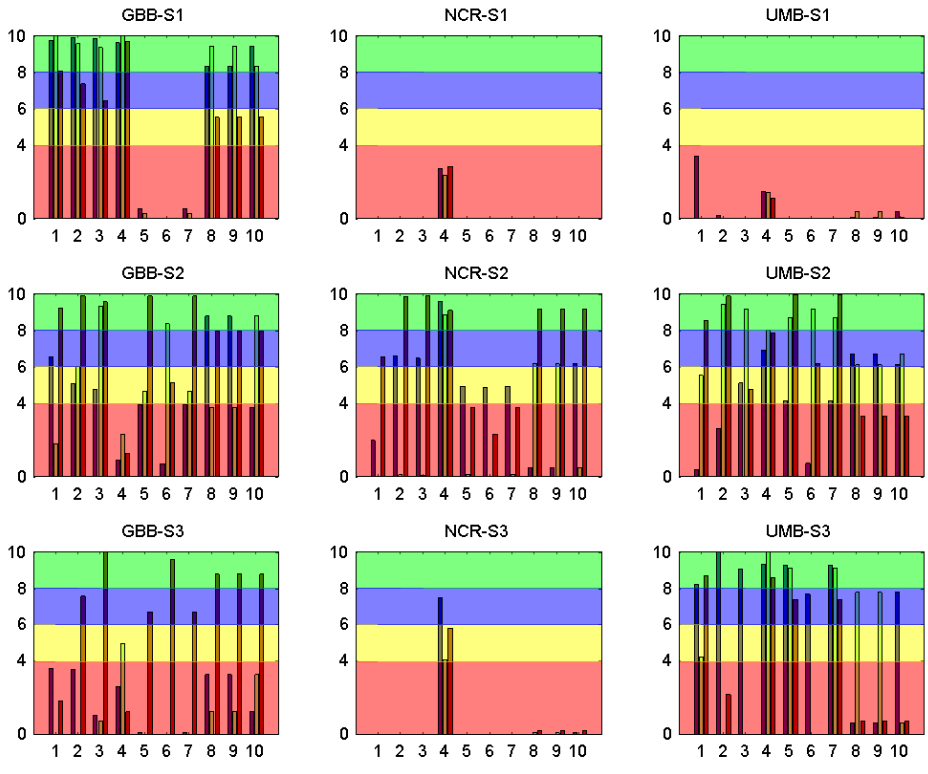

Figure 3.1. Misfit parameters (Anderson, 2004) of simulated ground motion at three strong motion stations: GBB (left), NCR (center), UMB (right) in the frequency band between 0.40 and 2.00 Hz. The results are shown for the three scenarios (S1: top panel; S2: center panel; S3: bottom panel) and the numbers used to indicate the

parameters are the following: 1 = PGA; 2 = PGV; 3 = PGD; 4 = Duration; 5 = Arias; 6 = Energy; 7= CAV; 8 = PSA; 9 = PSV; 10 = SD. Each parameter was estimated for three components.

Furthermore, Fig. 3.2 and 3.3 illustrate the comparison between recordings (blue) and synthetics (red) at the three strong motion stations under consideration in terms of displacement time histories and corresponding Fourier amplitude spectra, respectively.
It is noted that the numerical simulations are able to reproduce the most significant features of observed ground motion. The horizontal components of synthetic waveforms are in satisfactory agreement with the observations in terms of both major phases and the later arrivals. However, referring to the vertical component, numerical simulations tend to overestimate the recordings.

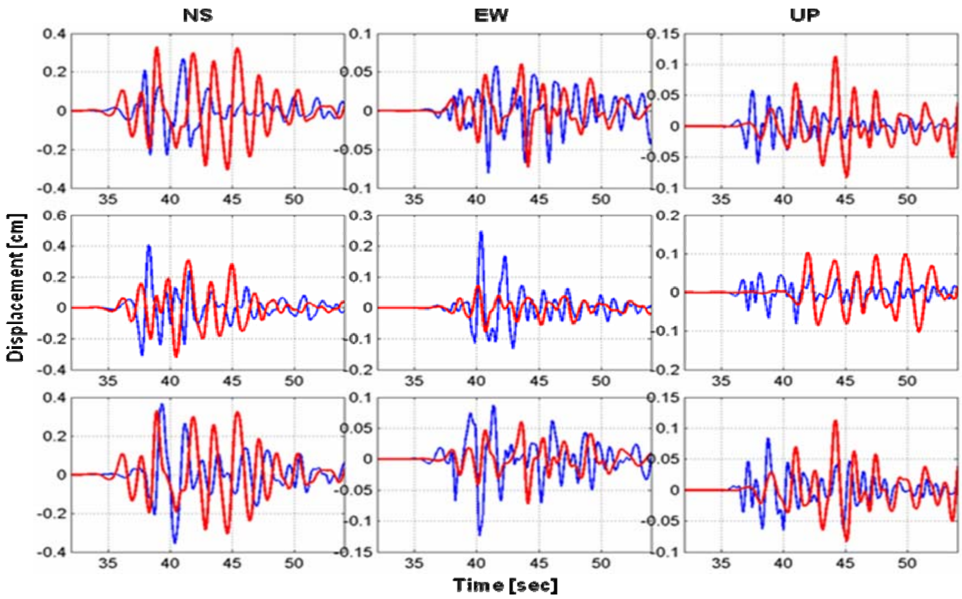

Figure 3.2. Comparison between strong-motion records (blue) and synthetic waveforms (red) from S2 at three stations (GBB: top panel; NCR: center panel; UMB: bottom panel). The displacement waveforms are band-pass filtered between 0.4 and 2.0 Hz.

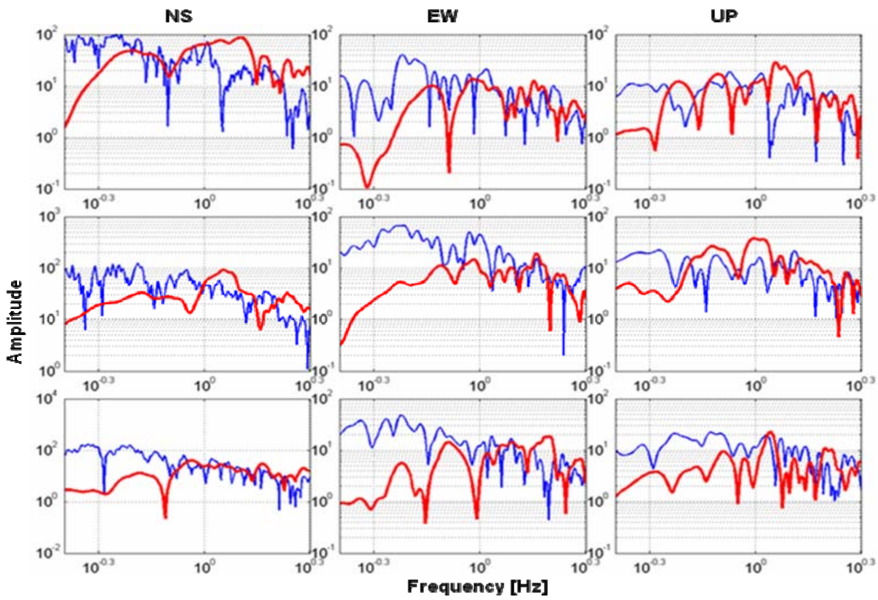

Figure 3.3. Same as in Fig. 3.2 in terms of Fourier amplitude spectra.

4. BASIN-EDGE EFFECTS

The pronounced dissimilarity in ground-motion characteristics between basin sites and nerby rocky sites has been widely studied during the past earthquakes in several basins. Significant ground motion amplification effects have been observed inside the Gubbio basin, as clearly attested by the strong motion records obtained at station GBP, located in the deeper part of the basin, during past earthquake sequences (see e.g. Pacor et al., 2007):

In order to study the effect of the basin structure on seismic motion, we analyze herein the results of numerical simulations (S2) obtained at GBP, if compared to those at GBB, located at a nearby rock site. The velocity time-histories and the 5% damped pseudo velocity response spectra at GBP (red) and GBB (black) are compared in Fig. 4.1. The differences between the simulated waveforms at GBP and GBB are remarkable, both in terms of peak ground velocity (PGV increases by a factor of about 5 passing from GBP to GBB) and significant duration. Further, the spectral response is considerably higher across all periods for GBP.

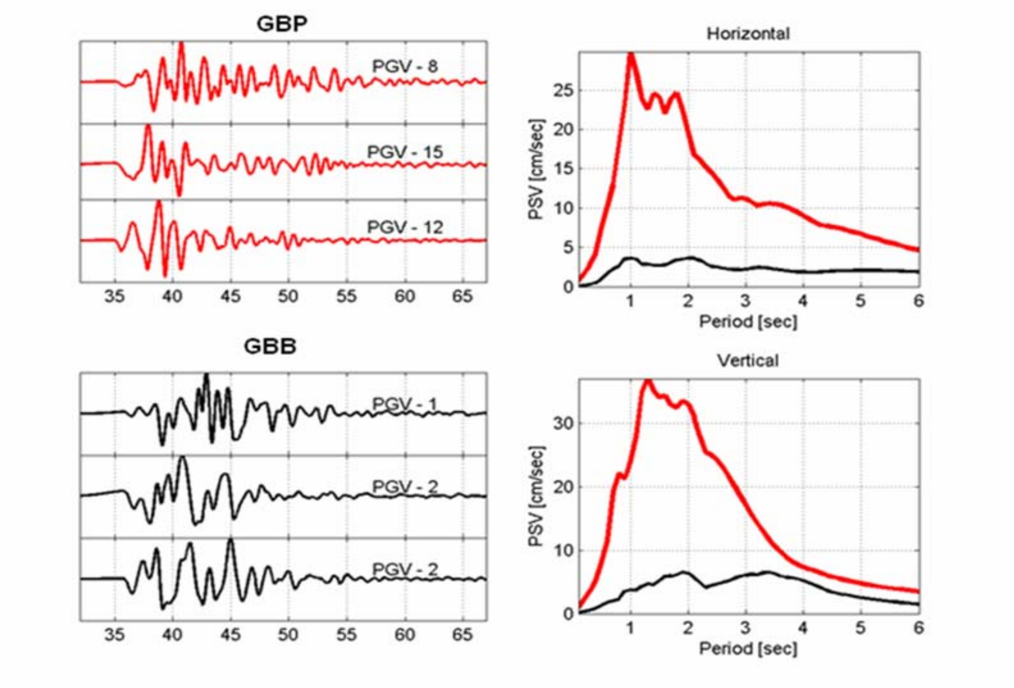

Figure 4.1. Comparison between GBP (red) and GBB (black) in terms of velocity time histories and 5% damped pseudovelocity response spectra as obtained from numerical simulations for S2. The time-series are arranged in left panels in the sequence of NS, EW and vertical components and the horizontal pseudo spectral velocity was computed as the geometric mean of NS and EW components.

From the comparison illustrated above, it is clear that the basin has significant influence on ground-motion characteristics. To further investigate this issue, the 1D analytical transfer function for the seismic response at GBP with respect to outcropping bedrock motion was estimated using the classical Haskell-Thomson matrix approach (Thomson 1950; Haskell 1953) and compared with the amplification function, as estimated from numerical simulations. The latter was computed as the ratio of the smoothed Fourier spectrum of the simulated waveform at GBP over that obtained at GBB. The comparison between the 1D theoretical and 3D numerical amplification function is illustrated in Fig. 4.2 for vertical motion. It is clear that the one-dimensional model is not capable of accounting for the large amplification on seismic ground motion in complex 3D structures. Ground motion amplification effects in the low frequency range, below 0.2 Hz, are reasonably due to complex site effects related to basin-edge induced surface waves.

In the following discussion, we will explore this issue in detail. The surface waves are dispersive in nature; we estimated the group velocity (*group velocity = distance/arrival time*) using the response envelope spectrum (RES) which is analogous to the multiple filtering. It was considered that the time at which the maximum spectral velocity attained was the *arrival time* for the corresponding period and similar operations were carried out for the periods of our interest. The estimated average dispersion curves for the receivers in the basin along with the standard deviation are plotted in Fig. 4.3 for the three different scenarios. We utilized vertical component motion for estimating the dispersion curve, therefore the resulting curve belongs to the Rayleigh vertical component. According to these dispersion curves, the dispersion seems nominal and the error bar indicates wider scattering in the estimate. It is interesting to see the larger group velocity for the long-period motion, because the longer period waves travel faster because of their longer wavelength, therefore, they travel through the deeper layers (higher velocity), while high frequency waves are primarily influenced by top layers which have low shear wave velocities, therefore travel slower than the long-periods. A fair trend observed in the dispersion curves is that the dispersion is appreciable between period 3 and 6 s with velocity ranging between 1000 to 1400 km/s.

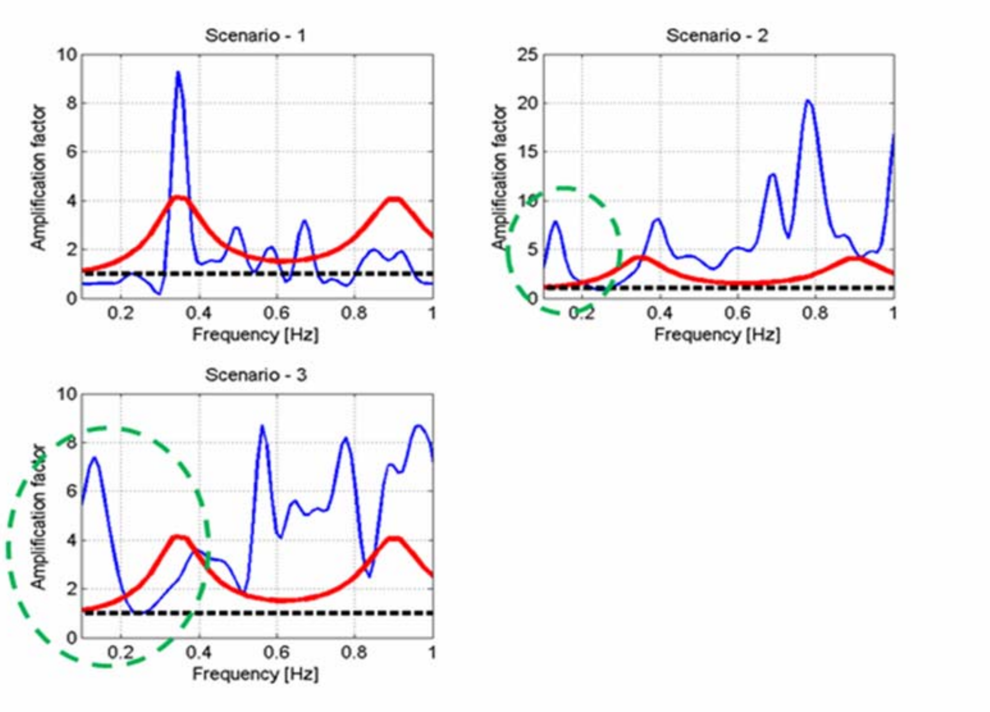

Figure 4.2. Comparison between the analytical 1D transfer function and the spectral ratio GBP/GBB as estimated from numerical simulations.

The isolation of surface waves in the strong-motion scenario could be a major challenge especially in the near field. Over great distances, the various wave types tend to become naturally separated due to dispersion effects, whilst no such separation usually occurs for strong motion recordings due to the proximity of the source. Seldom significant separation is noted in time domain but an appreciable segregation in frequency domain has been observed. Therefore, a band-pass filtering targeting the surface wave band would yield the desired results. From the above discussion, it is safe to conclude that the surface waves are expected be significant between periods 3 and 6 seconds due to the dispersion and larger amplification. Hence, we band-passed the motion between periods 3 and 6 seconds, the resulting motion from the radial, vertical and transverse components were considered to be Rayleigh horizontal, Rayleigh vertical and Love waves respectively. In Fig. 4.4, we have illustrated the hodogram for Rayleigh wave motion from 9 receivers; the particle motion follows elliptical motions fairly well which is the key character of the Rayleigh waves which gives us the confidence to further investigate the surface waves.

It would be an interesting result to quantify the contribution of surface waves to the total motion, in order to do that the energy carried by the seismic waves was estimated by the integral of squared velocity. The normalized energy was computed considering the entire record (0.1 – 2 Hz) and the 0.17

– 0.33 Hz pass band filtered surface wave signal. Fig. 4.5 shows the percentage of energy carried by Love and Rayleigh waves to total energy carried by the simulated motions. The mean percentage of surface waves is around 12%, and among the three scenarios, S3 is found to generate the most significant contribution (60%) of surface waves.

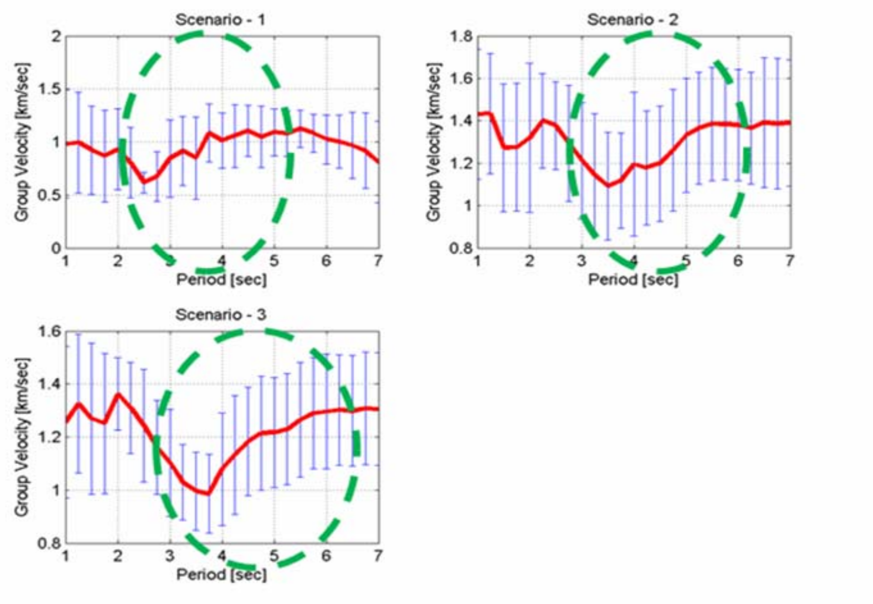

Figure 4.3. Dispersion curves for Rayleigh vertical component.

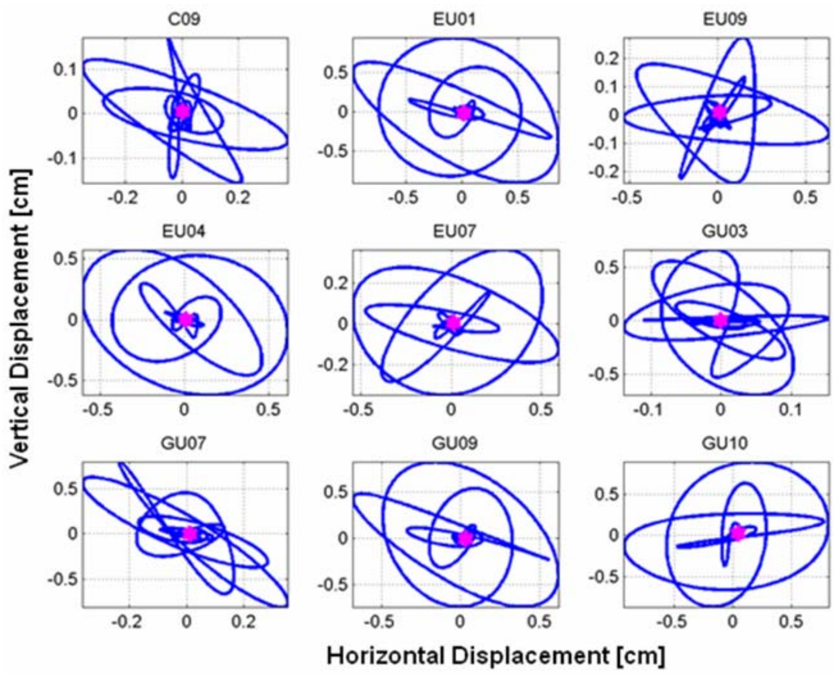

Figure 4.4. The particle motion plots (hodograms) of Rayleigh waves from S2 simualations.

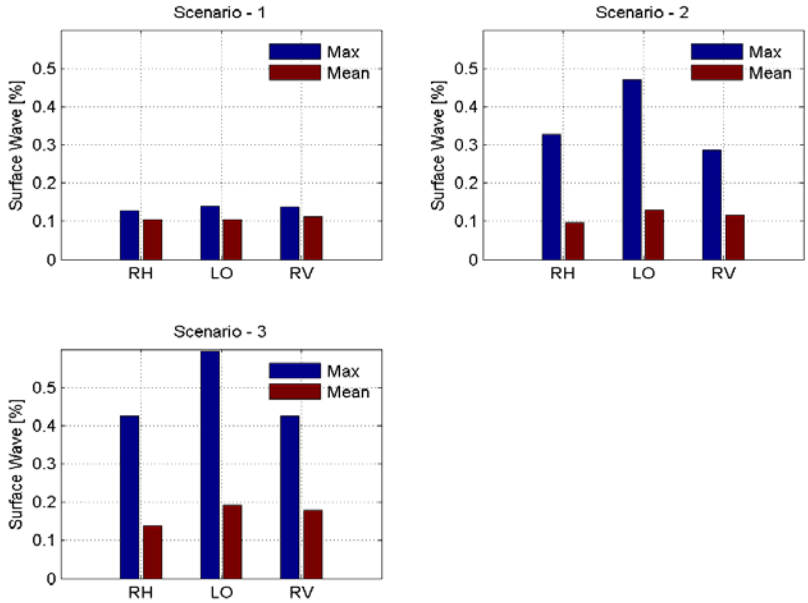

Figure 4.5. Percentage of energy carried by surface waves (RH = Rayleigh horizontal; LO = Love; RV = Rayleigh vertical) to the total energy

5. CONCLUSIONS

In this contribution we have shown the main results of 3D numerical simulations of earthquake ground motion in the Gubbio basin (Central Italy) during the M_W 5.7 1984 earthquake. Numerical simulations were carried out using the spectral element code GeoELSE, taking advantage of its implementation in parallel computer architectures. It turns out that the simulated ground motions are in reasonable agreement with the available strong motion recordings up to frequencies of about 2 Hz, so that the numerical model can be used to simulate a possible future M_W 6 event occurring on the northern segment of the Gubbio fault with a larger degree of confidence.

The three-dimensional numerical simulations provide interesting insights into complex effects of seismic wave propagation related to the generation of surface waves in complex geomorphological structures such as the Gubbio basin. Relying on the results of numerical simulations, previously validated against strong motion observations, the main features of ground motion amplification inside the Gubbio basin have been investigated. With this objective, the following tasks have been achieved:

- the low frequency amplification observed in the basin sites owing to the generation of surface waves at the basin edges cannot be fully accounted for through standard 1D approach for local seismic response.
- The dispersion curves were estimated using Rensponse Envelope Spectrum (RES), suggesting that surface waves carry significant energy in the periods between 3 and 6 s.
- Surface waves were isolated using suitable band-pass filters and later validated with the hodogram plots; around 12% of the total motion is found to be associated with surface waves.
- The generation of surface waves turns out to depend on seismic source parameters, such as hypocenter location and rise time. It is found that the earthquake scenario with lower rise time and shallower focal depth leads to larger surface wave contributions.

AKCNOWLEDGEMENT

We deeply thank Gabriele Ameri for providing the data regarding the slip distribution. The authors are very grateful to the Consorzio Interuniversitario Lombardo per L'Elaborazione Automatica (CILEA), in Milan, for allowing the access to the Lagrange cluster.

REFERENCES

Ameri, G., Gallovič, F. Pacor,F. and Emolo, A. (2010). Uncertainties in Strong Ground-Motion Prediction with Finite-Fault Synthetic Seismograms: An Application to the 1984 M 5.7 Gubbio,Central Italy, Earthquake. *Bull. Seismol. Soc. Am.* **99**,647-663.

Anderson J.G. (2004) Quantitative measure of the goodness fit of synthetic seismograms. In Proceedings of the 13th World Conference on Earthquake Engineering, Vancouver, B.C., Canada, Paper no. **243**.

Archuleta, R.J. and Hartzell, S.H. (1981) Effects of fault finiteness on near-source ground motion. *Bull. Seismol. Soc. Am.* **71:4**, 939–957.

Bindi D, Parolai S, Cara F, Di Giulio G, Ferretti G, Luzi L, MonachesiG, Pacor F, RovelliA (2009) Site amplification observed in the Gubbio basin, Central Italy: hints for lateral propagation effects. *Bull Seismol Soc Am* **99:2A**,741–760

Bray, J.D. and Rodriguez-Marek, A. [2004] Characterization of forward-directivity ground motions in the near-fault region. *Soil Dyn. Earthq. Eng.* **24:11**, 815–828.

Collettini C., Barchi M., Chiaraluce L., Mirabella F., and Pucci S. (2003). The Gubbio fault: can different methods give pictures of the same object? *Journal of Geodynamics* **36**, 51-66.

DISS Working Group (2009) *Database of Individual Seismogenic Sources (DISS), Version 3.1.0: A compilation of potential sources for earthquakes larger than M 5.5 in Italy and surrounding areas*. Technical report, Istituto Nazionale di Geofisica e Vulcanologia (INGV).

Faccioli E., F. Maggio, R. Paolucci and A. Quarteroni. (1997) 2D and 3D elastic wave propagation by a pseudo-spectral domain decomposition method *Journal of Seismology* **1**, 237-251

Haskell NA (1953) The dispersion of surface waves on multilayered media. *Bull Seismol Soc Am* **43:1**,17

Hernandez B, Cocco M, Cotton F, Stramondo S, Scotti O, CourboulexF Campillo M, Campillo F (2004) Rupture history of the 1997 Umbria-Marche (Central Italy) main shocks from the inversion of GPS, DInSAR and near field strong motion data. *Ann Geophys*, **47,**1355–1376

Koketsu KM, Miyake H (2008) A seismological overview of long-period ground motion. *J Seismol* **12**, 133-143.

Mirabella F, Ciaccio MG, Barchi MR, Merlini S (2004) The Gubbio normal fault (Central Italy): geometry, displacement distribution and tectonic evolution. *J Struct Geol* **26**, 2233–2249

Pacor F., D. Bindi , L. Luzi , S. Parolai, S. Marzorati and G. Monachesi (2007),Characteristics of strong ground motion data recorded in the Gubbio sedimentary basin (Central Italy), *Bull Earthquake Eng* **5**, 27-43.

Pucci S, De Martini M, Pantosti D, Valensise G (2003) Geomorphology of the Gubbio basin (Central Italy): understanding the active tectonics and earthquake potential. *Ann Geophys* **46:5**,837–864

Smerzini, C., Paolucci, P. ·and Stupazzini M. (2010).Comparison of 3D, 2D and 1D numerical approaches to predict long period earthquake ground motion in the Gubbio plain, Central Italy. *Bull Earthquake Eng* **9:6**, 2007 – 2029.

Somerville, P. G., Smith, N. F., Graves, R. W., and Abrahamson, N. A.. (1997) Modification of empirical strong ground motion attenuation relations to include the amplitude and duration effects of rupture directivity *Seismol. Res. Lett.,* **68**, 199-222.

Stupazzini, M., Paolucci, R. and Igel, H. (2009). Near-Fault Earthquake Ground-Motion Simulation in the Grenoble Valley by a High-Performance Spectral Element Code. *Bull. Seism. Soc. Am.* **99**: 286-301.

Thomson WT (1950) Transmission of elastic waves trough a stratified solid medium. *J Appl Phys* **21**,89–93